

Electrochemical characteristics of phosphorus doped Si-C composite for anode active material of lithium secondary batteries

Jae-Hyun NOH^{1,2}, Kwan-Young LEE², Joong-Kee LEE¹

1. Battery Research Center, Korea Institute of Science and Technology, P.O. Box 131, Cheongryang, Seoul, 130-650, Korea;

2. Department of Chemical and Biological Engineering, Korea University, Seoul, 136-791, Korea

Received 18 June 2008; accepted 10 March 2009

Abstract: Phosphorus doped silicon-carbon composite particles were synthesized through a DC arc plasma torch. Silane(SiH₄) and methane(CH₄) were introduced into the reaction chamber as the precursor of silicon and carbon, respectively. Phosphine(PH₃) was used as a phosphorus dopant gas. Characterization of synthesized particles were carried out by scanning electron microscopy(SEM), X-ray diffractometry(XRD), X-ray photoelectron spectroscopy(XPS) and bulk resistivity measurement. Electrochemical properties were investigated by cyclic test and electrochemical voltage spectroscopy(EVS). In the experimental range, phosphorus doped silicon-carbon composite electrode exhibits enhanced cycle performance than intrinsic silicon and phosphorus doped silicon. It can be explained that incorporation of carbon into silicon acts as a buffer matrix and phosphorus doping plays an important role to enhance the conductivity of the electrode, which leads to the improvement of the cycle performance of the cell.

Key words: secondary batteries; anode; silicon-carbon composite; phosphorus doping; arc plasma pyrolysis

1 Introduction

Carbonaceous materials are commercially used for anode materials of lithium-ion secondary batteries. These carbonaceous materials give good cycling performance due to lithium intercalation-deintercalation mechanism. However, the theoretical maximum capacity of these materials is only 372 mA·h/g[1–2]. Silicon based materials have been studied as alternative anode materials for lithium secondary batteries due to high theoretical capacity (4 200 mA·h/g) and high energy density. However, silicon based materials have several problems as follows: 1) drastic volume change (>400%) during the alloying and de-alloying reaction which leads to remarkably rapid capacity fading of the electrode caused by breakdown of the electrode[3–4]; and 2) low electrical conductivity of silicon itself. Many studies have been carried out to improve the electrochemical performance and minimize the mechanical stress caused by the large volume change of silicon based materials. Several approaches such as “active-inactive”[5–8], “nano-composites” “core-shell”[9–10] have been employed to solve the above intractable problem for the

metal-based materials for the electrode of lithium-ion batteries[11]. In the case of “active-inactive”, dual-phase composites consisted of active Si and inactive materials such as Sn-Fe-C, Si-SiC, Si-TiC and Si-TiB₂ are used [12–17]. In these systems, the inactive phase acts as a buffering matrix with good mechanical properties and it improves quite the reversible capacity and cyclability.

Another way to solve the above problems is enhancing the electrical conductivity of silicon particles. This is because increased electrical conductivity reduces contact and charge-transfer resistances during charging-discharging reaction between interparticles interface, resulting in the improved Li de-alloying kinetics[18]. KOMABA et al[19] reported the effect of phosphorus doped n-type silicon. They demonstrated that the enhancement of electric conductivity caused by phosphorus doping results in the improved cycle performance using the thin film electrode.

In this study, effects of phosphorus doping into silicon particles and incorporation of carbon into doped silicon on electrochemical performance of the anode materials of lithium secondary batteries were investigated.

2 Experimental

Three different silicon based materials, i.e., intrinsic silicon, phosphorus doped silicon, and phosphorus doped silicon-carbon composite were prepared using DC arc plasma torch. Silane of 50 mL/min, 5% phosphine/balance Ar of 10 mL/min and methane of 20 mL/min used as the precursor of silicon, phosphorus and carbon, respectively, were introduced into the reaction chamber through the gas mixing tube. Therefore, phosphorus atoms present at 1% of silicon atoms in synthesized particles. The plasma generating power was kept constant at 4 kW (200 A/20 V). The synthesized particles were characterized by X-ray diffractometry(XRD), X-ray photoelectron microscopy(XPS) and bulk resistance measurement.

The anode electrodes were prepared by mixing 40% (mass fraction) active materials with 40% carbon black and 20% polyvinylidene fluoride(PVDF) dissolved in *N*-methyl pyrrolidinone(NMP). The slurry was spread on 10 μm -thick copper foil and dried at 80 $^{\circ}\text{C}$ for 1 h. The electrode was pressed using rolling press at 120 $^{\circ}\text{C}$ and was dried in vacuum oven at 80 $^{\circ}\text{C}$ for overnight. The half cells were fabricated into pouch type including the Li metal foil, separator and electrolyte in dry room (maximum moisture <5%). The electrolyte of 1 mol/L LiPF_6 dissolved in a 1:1:1 (volume ratio) mixture of ethylene carbonate(EC), ethyl-methyl carbonate(EMC) and dimethyl carbonate(DMC) was employed. The electrochemical properties of fabricated half cells were characterized by galvanostatic method. The cycling was carried out at constant current density of 0.1C and cutoff voltage of 2.0 V vs Li/Li^+ .

3 Results and discussion

Fig.1 shows XRD patterns of intrinsic silicon and phosphorus doped silicon-carbon composite. In the case of intrinsic silicon shown in Fig.1(a), only diffraction peaks related to (111), (220), (311), (400) and (311) of poly-crystalline silicon are presented. The diffraction peaks of phosphorus doped silicon are shown in Fig.1(b). It is observed that the phosphorus doped silicon has lower peak intensity than undoped one. The intensity of each peak is caused by the crystallographic structure, the position of the atoms within the elementary cell and their thermal vibration. There is not any difference in view of the crystallographic structure because 2θ angles of two patterns are almost same. This means that lower peak intensity of phosphorus doped silicon is attributed to changing of thermal vibration by adding phosphorus atoms. On the other hand, in the case of phosphorus

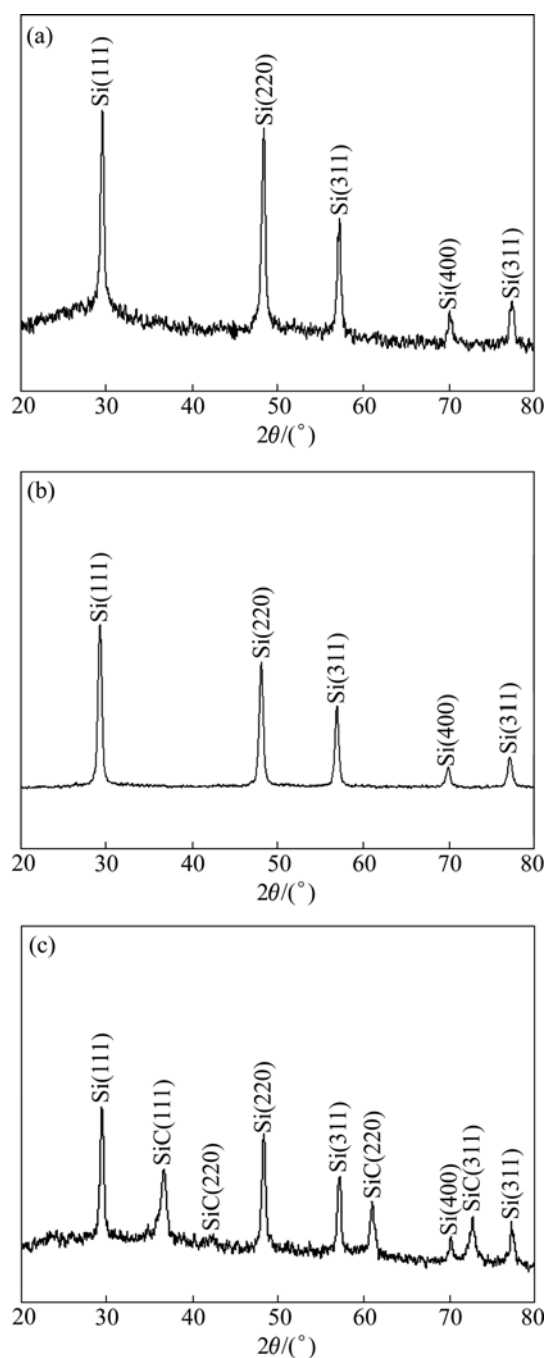


Fig.1 XRD patterns for intrinsic silicon (a), phosphorus doped silicon (b) and phosphorus doped silicon-carbon composite (c)

doped silicon-carbon composite shown in Fig.1(c), some of the diffraction peaks related to β -SiC phase corresponding to the angles of $2\theta=36.7^\circ$, 60.7° and 72.4° are observed. The above results indicate that incorporation of carbon into silicon causes the formation of SiC. Synthesized phosphorus doped silicon-carbon composite particles are composed of Si as active material and SiC as inactive matrix with lithium.

XPS analysis was carried out to investigate the bonding status of phosphorus and silicon for phosphorus

doped silicon-carbon composite. Fig.2(a) shows Si 2p spectra. The SiO₂, Si—Si, Si—C and Si—C—O peaks corresponding to 102.5, 98.3, 99.8 and 101.3 eV are observed in Si 2p. And P—P bond at 129.5 eV and P₂O₅ bond at 133 eV are found in P 2p₃ in Fig.2(b). The presence of peaks related to phosphorus is found by XPS analysis and it is expected to be caused by phosphorus as a dopant.

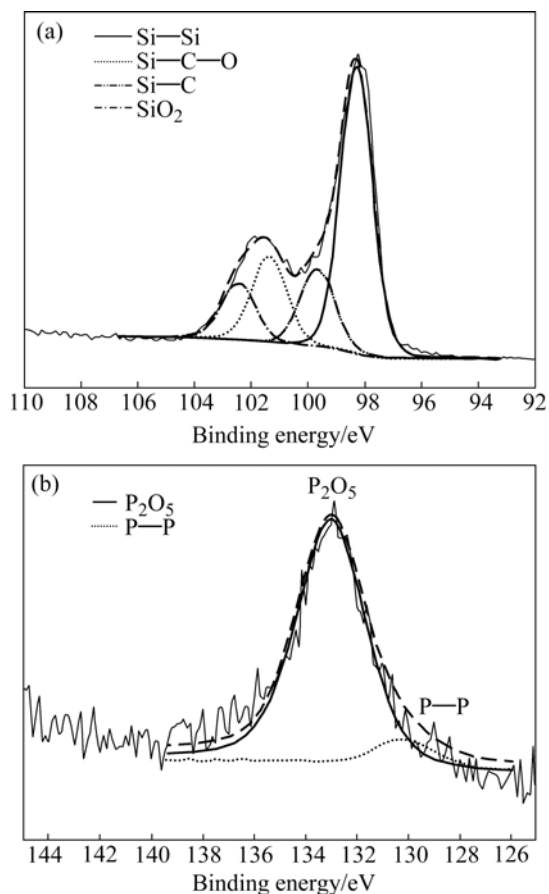


Fig.2 XPS spectra of phosphorus doped silicon-carbon composite for Si 2p (a) and P 2p₃ (b)

Electrical bulk resistivity of each sample was measured by a 4-point-probe tool. Fig.3 shows the results of measurement. Intrinsic silicon shows the highest electrical bulk resistivity among the samples. In the case of phosphorus doped silicon, electrical bulk resistivity is decreased in comparison with the undoped one. It is expected that phosphorus atoms act as dopant in silicon lattice structure. On the other hand, phosphorus doped silicon-carbon composite indicates higher electrical bulk resistivity than phosphorus doped silicon. It seems that Si—C bonds in phosphorus doped silicon-carbon composite makes the electrical conductivity lower due to wide band energy and low hall mobility.

In Fig.4 the cyclic behaviors of three different silicon based materials are compared. And the discharge capacities at initial cycle after 30 cycles and capacity

retention of each samples are given in Table 1. In this work, acetylene black (AB) used as the conductor has about 150 mA/g of specific capacity, which should be considered because of the higher mass ratio (40%). Thus, the capacity induced by the acetylene black will be deducted from Fig.4 and Table 1[12]. The first discharge capacities of intrinsic silicon, phosphorus doped silicon and phosphorus doped silicon-carbon composite are 2 365, 1 782 and 1 087 mA·h/g, respectively. This obviously indicates that phosphorus doped silicon-carbon composite exhibits the lowest first discharge capacity among the samples. It seems that phosphorus doping effect and formation of SiC result in capacity loss due to inactivity of phosphorus and SiC with lithium. The electrode made from intrinsic silicon shows a rapid capacity fading and its discharge capacity after 30 cycles is retained only 2% of initial discharge capacity. However, in the case of phosphorus doped silicon, the cyclic performance is somewhat improved in comparison with intrinsic silicon. The discharge capacity after 30

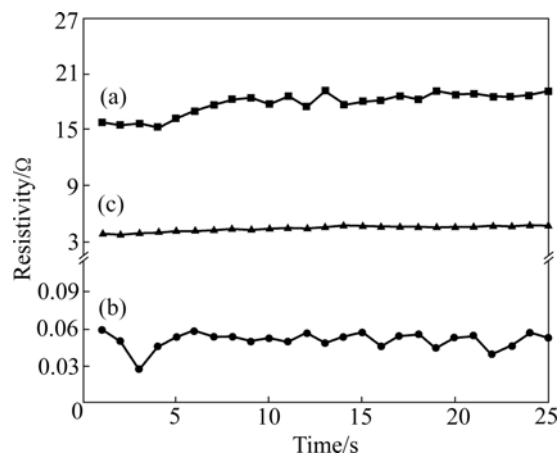


Fig.3 Electrical bulk resistivity of intrinsic silicon (a), phosphorus doped silicon (b) and phosphorus doped silicon-carbon composite (c)

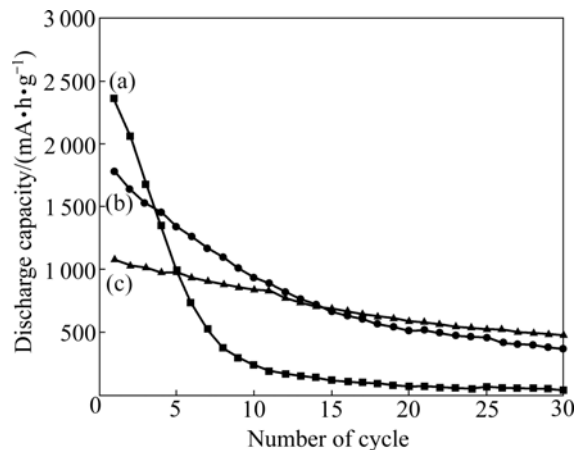


Fig.4 Cyclic performance of intrinsic silicon (a), phosphorus doped silicon (b) and phosphorus doped silicon-carbon composite (c)

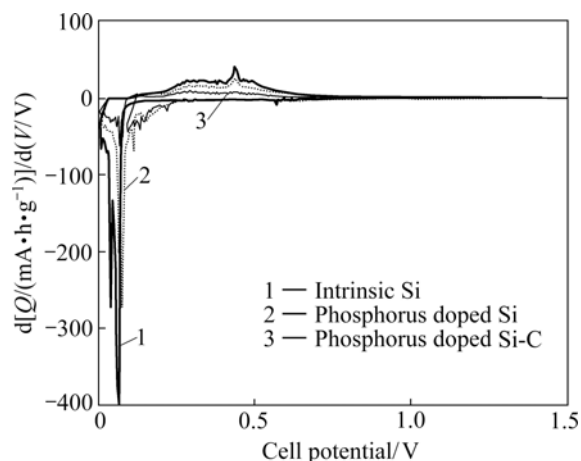
Table 1 Discharge capacities at initial cycle and after 30 cycles and capacity retention

Material	Initial discharge capacity/ (mA·h·g ⁻¹)	Discharge capacity after 30 cycles/ (mA·h·g ⁻¹)	Capacity retention after 30 cycles/%
Intrinsic silicon	2 365	49	2
P doped Si	1 782	376	21
P doped Si-C	1 087	484	45

cycles of phosphorus doped silicon is retained about 21% of initial discharge capacity.

The improvement is due to the enhancement of electric conductivity by the phosphorus doping, which maintains the electric contact and provides sufficient electric field within the electrode during the charging-discharging reaction, resulting in improved Li de-alloying kinetics[18]. Moreover, phosphorus doped silicon-carbon composite exhibits much increased reversible capacity and improved capacity retention after 30 cycles with values of 544 mA·h/g and 45%, respectively. This suggests that SiC particles act as inactive buffer matrix, which can reduce cracking and pulverization of the electrode[13–14].

The differential capacities of intrinsic silicon, phosphorus doped silicon and phosphorus doped silicon-carbon composite at first cycle are shown in Fig.5. In first lithiation reaction, the intrinsic silicon exhibits sharp anodic peak around 0.1 V, which is attributed to the lithium alloy formation with silicon. However, in the case of the doped samples, there appears broad anodic peak over wide voltage range below 0.3 V. It seems that the crystal structure of the silicon undergoes change of the crystallinity because phosphorus atoms penetrate into the silicon lattices. On the other hand, the phosphorus doped silicon-carbon composite shows very similar peaks in comparison with phosphorus doped silicon. This suggests that SiC particles are unrelated with electro-

**Fig.5** Differential capacity plots of intrinsic silicon, phosphorus doped silicon and phosphorus doped silicon-carbon composite

chemical reaction as inactive matrix component, but play an important role as a buffer matrix during charging-discharging process[13–14].

4 Conclusions

1) Three different samples, intrinsic silicon, phosphorus doped silicon and phosphorus doped silicon-carbon composite were synthesized by plasma arc discharge method and they were used for the anode for lithium secondary batteries in order to investigate the effects of carbon and phosphorus doping into silicon on electrochemical performance for the anode materials of lithium secondary batteries. It is expected that the composite provides enhanced cyclic performance due to synergetic effect of the excellent buffering matrix behavior of carbon and increase of electrical conductivity of silicon material from phosphorus doping.

2) The cells were assembled to pouch type and were galvanostatically charged and discharged in the voltage range of 0–2 V vs Li/Li⁺ at a constant current density of 30 mA·h/g. The results explain that phosphorus doped silicon-carbon composite shows better performance in cycle stability than intrinsic silicon and phosphorus doped silicon. The carbon acts as buffering matrix for volumetric change of silicon during alloying and de-alloying. The phosphorus doping plays a role to keep the potential uniformity of the electrode. The phosphorus doped carbon-silicon shows the highest capacity retention, 45% of initial capacity after 30 cycles. On the other hand, the intrinsic silicon and phosphorus doped silicon show 2% and 21% of capacity retention, respectively.

Acknowledgement

This research was supported by a grant (code #05K1501-01920) from ‘Center for Nanostructured Materials Technology’ under ‘21st Century Frontier R&D Programs’ of the Ministry of Science and Technology, Korea.

References

- [1] YANG X Q, MCBEEN J, YOON W S, YOSHIO M, WANG H, FUKUDA K, UMENO T. Structural studies of the new carbon-coated silicon anode materials using synchrotron-based in situ XRD [J]. *Electrochem Commun*, 2002, 4: 893–897.
- [2] GUO Z P, WANG J Z, LIU H K, DOU S X. Study of silicon/polypyrrole composite as anode materials for Li-ion batteries [J]. *J Power Sources*, 2005, 146: 488–451.
- [3] YANG X, WEN Z, ZHU X, HUANG S. Preparation and electrochemical properties of silicon/carbon composite electrodes [J]. *Electrochem Solid-State Letter*, 2005, 8: A481–A483.
- [4] GRAETZ J, AHN C C, YAZAMI R, FULTZ B. Highly reversible lithium storage in nanostructured silicon [J]. *Electrochem Solid-State Lett*, 2003, 6: A194–A197.

- [5] LEE H Y, JANG S W, LEE S M, LEE S J, BAIK H K. Lithium storage properties of nanocrystalline Ni_3Sn_4 alloys prepared by mechanical alloying [J]. *J Power Sources*, 2002, 112: 8–12.
- [6] UEHARA M, SUZUKI J, TAMURA K, SEKINE K, TAKAMURA T. Thick vacuum deposited silicon films suitable for the anode of Li-ion battery [J]. *J Power Sources*, 2005, 146: 441–444.
- [7] KIM H, PARK B, SOHN H J, KANG T. Electrochemical characteristics of Mg-Ni alloys as anode materials for secondary Li batteries [J]. *J Power Sources*, 2000, 90: 59–63.
- [8] KIM B C, UONO H, SATO T, FUSE T, ISHIHARA T, SENNA M. Li-ion battery anode properties of Si-carbon nanocomposites fabricated by high energy multiring-type mill [J]. *Solid State Ionics*, 2004, 172: 33–37.
- [9] DIMOV N, KUGINO S, YOSHIO M. Carbon coating silicon as anode as material for lithium ion batteries: Advantages and limitations [J]. *Electrochim Acta*, 2003, 48: 1579–1587.
- [10] WILLSON A M, WAY B M, DAHN J R. Nanodispersed silicon in pregraphitic carbons [J]. *J Appl Phys*, 1995, 77: 2363–2369.
- [11] ZUO P, YIN G, MA Y. Electrochemical stability of silicon/carbon composite anode for lithium ion batteries [J]. *Electrochim Acta*, 2007, 52: 4878–4883.
- [12] ZHANG X N, PAN G L, LI G R, QU J Q, GAO X P. Si- Si_3N_4 composites as anode materials for lithium ion batteries [J]. *Solid State Ionics*, 2007, 178: 1107–1112.
- [13] KIM I S, BIOMGREN G E, KUMTA P N. Si-SiC nanocomposite anodes synthesized using high-energy mechanical milling [J]. *J Power Sources*, 2004, 130: 275–280.
- [14] WARD D A, KO E I. Preparing catalytic materials by the sol-gel method [J]. *Ind Eng Chem Res*, 1995, 34: 421–433.
- [15] PATEL P, KIM I S, KUMTA P N. Nanocomposites of silicon/titanium carbide synthesized using high-energy mechanical milling for use as anodes in lithium-ion batteries [J]. *Mater Sci Eng B, Solid-State Mater Adv Technol*, 2005, 116: 347.
- [16] GUO Z P, ZHAO Z W, LIU H K, DOU S X. Lithium insertion in Si-TiC nanocomposite materials produced by high-energy mechanical milling [J]. *J Power Sources*, 2005, 146: 190–194.
- [17] KIM I S, BIOMGREN G E, KUMTA P N. Nanostructured Si/TiB₂ composite anodes for Li-ion batteries [J]. *Electrochim Solid-State Lett*, 2003, 6: A157–A161.
- [18] KIM J W, RYU J H, LEE K T, OH S M. Improvement of silicon powder negative electrodes by copper electroless deposition for lithium secondary batteries [J]. *J Power Sources*, 2005, 147: 227–233.
- [19] KOMABA S, MIKAMI F, ITABASHI T, BABA M, UENO T, KUMAGAI N. Improvement of electrochemical capability of sputtered silicon film anode for rechargeable lithium batteries [J]. *Bull Chem Soc Jpn*, 2006, 79: 154–162.

(Edited by YANG Bing)